



# VIBRATION PROTECTION OF CRITICAL COMPONENTS OF ELECTRONIC EQUIPMENT IN HARSH ENVIRONMENTAL CONDITIONS

A. M. VEPRIK

*Wolfson School of Mechanical and Manufacturing Engineering, Loughborough University,  
Leicestershire LE11 3TU, England. E-mail: a.veprik@lboro.ac.uk*

*(Received 17 August 2001, and in final form 7 January 2002)*

Vibration protection of sensitive electronic equipment operating in harsh environments often relies on resilient mounts. The traditional optimal design for vibration isolation from random vibration is based on a trade-off choice of damping and stiffness properties of mounts, and is focussed primarily on optimizing the dynamic response of the electronic boxes, subject to limitations imposed on their rattle space. However, the reliability of the electronic equipment depends primarily on the vibration responses of the internal components that are often lightly damped and extremely responsive over a wide frequency range. The traditional approach, hence, completely ignores the presence of such components. Consequently, the traditionally designed vibration isolators are often insufficient for maintaining a fail-safe vibration environment for electronic equipment. The new design approach focuses basically on dynamic properties and responses of the critical internal components of an electronic device. The optimally chosen elastic and damping properties of the vibration isolators allow the vibration experienced by the above internal components to be minimised, subject to restraints imposed on the peak deflections of the electronic box.

© 2002 Published by Elsevier Science Ltd.

## 1. INTRODUCTION

Modern electronic equipment, which is used widely in military applications, must be able to survive harsh environmental conditions for the life cycle in excess of 20 years. The endurance of such equipment is defined primarily by the ability of their internal sensitive components, e.g., printed circuit boards (PCB), to survive severe vibration without developing the critical fatigue to the mounted components, soldered joints, connectors, etc., [1–3]. Traditionally, for increased survivability in a harsh environment, the PCBs are ruggedized using frames, frames with backplanes, stiffening ribs, etc., [2, 4, 5, see also examples given in APW Electronic Solutions Ltd website].<sup>†</sup>

Recently, there has been a significant improvement in the quality and durability of the low-cost commercial hardware followed by a trend within the defence industry to make use of commercial-off-the-shelf (COTS) components. The COTS initiative, which was launched in 1994 by William Perry, then U.S. Secretary of Defence, is aimed at abandoning, where possible, costly MIL-SPEC hardware [6–8]. This move is caused not only by the financial need originated by downsized military budgets in the post Cold War Era, but also by the opportunity for rapid access to the latest technologies.

<sup>†</sup><http://www.apw.com/productsServices/productShowcase/raptor462.jsp>

While much improved, COTS hardware sometimes appears not to be rugged enough to survive the environmental conditions encountered. The typical lifetime of the COTS electronics is 7–10 years [8] as opposed to 20 years, which is typical for their “military-borne” rivals. When reliability becomes a critical factor, the industry is moving back towards designs based on the strict military guidelines [9].

Considerable attempts have been made recently to implement the principle of vibration isolation of electronic equipment containing unmodified COTS PCBs. This approach involves location of the equipment in the shock and vibration isolated sub-chassis or modules [1,10–13, see also AP Lab<sup>‡</sup> examples]. Apparently, in spite of the fact that the electronic box is a complex, sometimes non-linear, dynamic structure containing sensitive internal components, the design for vibration isolation normally relies on the traditional simplified linear model of a flexurally suspended solid body, the theory of which is reasonably completed [14, 15].

Nonetheless, the attempts of vibration protection of the sensitive electronic hardware are regarded widely as something of a black art and require a great deal of experimental work to be done to find appropriate vibration isolators to protect a particular electronic box. An improperly designed vibration isolation arrangement can make matters worse and even cause damage, which would not otherwise have happened. This is, mainly, because the electronic device with sensitive internal components is not a traditional subject of vibration protection (six-degree-of-freedom flexurally suspended solid body). The apparent drawback of the above traditional approach is that when analysis of the isolation system is carried out, it is normally the dynamics of the internal sensitive components that is ignored and the dynamic response of the enclosure alone that is optimized [1–3,10–12,16,17, see also “Vibration and Shock Theory” by Lord Corporation<sup>§</sup>]. Such a concept absolutely misses the purpose of using isolators, which should be, in reality, the protection of the sensitive internal components from developing excessive dynamic responses.

The above traditional approach to vibration isolation calls for the application of inadequately heavily damped vibration isolators. Those are required primarily for the close control of peak deflections of the entire electronic enclosure under the worst combination of a wideband random excitation (e.g., flight through turbulent flow) and high  $g$ -loads experienced at take-off, climb, high-speed turn, speedup, etc. It is a widespread opinion, which is supported by the leading manufacturers of vibration isolators, that only highly damped isolation materials provide the only choice for adequate protection of electronic equipment [18].

Apparently, such an approach leads to vibration protection systems with poor isolation properties in the high-frequency range containing typical natural frequencies of the internal sensitive components, and which are often insufficient for maintaining a fail-safe vibration environment for delicate electronic equipment [19].

The theory of optimal vibration isolation for such complex systems does not appear to exist [14], and, as a matter of fact, the optimal system design procedure is not yet fully developed. Successful application of the principle of vibration isolation for COTS electronics requires enhancement of the model of the object of vibration protection by considering additional degrees of freedom reflecting the actual dynamic properties and responses of the internal sensitive components, and development of new approaches to the optimal design of such systems.

<sup>‡</sup> [http://www.sd.aplabs.com/enweb/Products/product\\_details.asp?Standard.ATR#FS7275](http://www.sd.aplabs.com/enweb/Products/product_details.asp?Standard.ATR#FS7275)

<sup>§</sup> [http://www.lordmpd.com/catalogs/aa\\_theory.asp](http://www.lordmpd.com/catalogs/aa_theory.asp)

This paper enhances the author's ideas [20–22]. The novel approach proposed is the use of vibration isolators with properties to minimize the dynamic response of internal sensitive components (PCB, in this instance), subject to the restraints imposed on the peak deflections of the entire electronic enclosure. This design approach utilizes the already existing heavy equipment box as the first level isolation stage relative to the light PCB.

## 2. ESTIMATION OF DYNAMIC PROPERTIES OF PCB

Our primary objective is to develop an approach to the optimal design of the vibration isolation system for the critical electronic equipment with focus on the control of the dynamic responses of the internal sensitive components. For this purpose, one needs now the dynamic properties of the typical PCB, which is used in this paper, to be estimated.

Figure 1 shows the schematics of the experimental rig. The PCB ①, which carries a flatpack chip, is mounted rigidly upon the fixture ②. The fixture is mounted upon the electrodynamic shaker ③ (vibration test system V550/PA550L, Ling Dynamic Systems Ltd.) perpendicularly to the direction of the motion. The shaker is driven using controller (model DVC 48, Ling Dynamic Systems Ltd) ④ and PC ⑤, where accelerometer (Bruel & Kjaer, Type 4393) ⑥ is used for the close-loop control. Another accelerometer ⑦ (Bruel & Kjaer, Type 4393) and conditioning amplifier ⑧ (Bruel & Kjaer, Type 2635) are used for measuring the absolute acceleration of the fixture. The fibre optic laser vibrometer ⑨ (Dual Beam Polytec OFV 512 Fibre Interferometer and OFV 3001 Vibrometer Controller) measures the absolute and relative response of the PCB. The portable signal analyser ⑩ (Signal Calc Ace, Data Physics Corporation) carries out the data acquisition and signal analysis and is connected to the PC via PCMCIA-II port.

Figure 2 shows the layout of the experimental rig. Figures 3 and 4 show the modules of experimentally measured complex universal absolute and relative transmissibilities, which are typical for COTS PCBs [1].

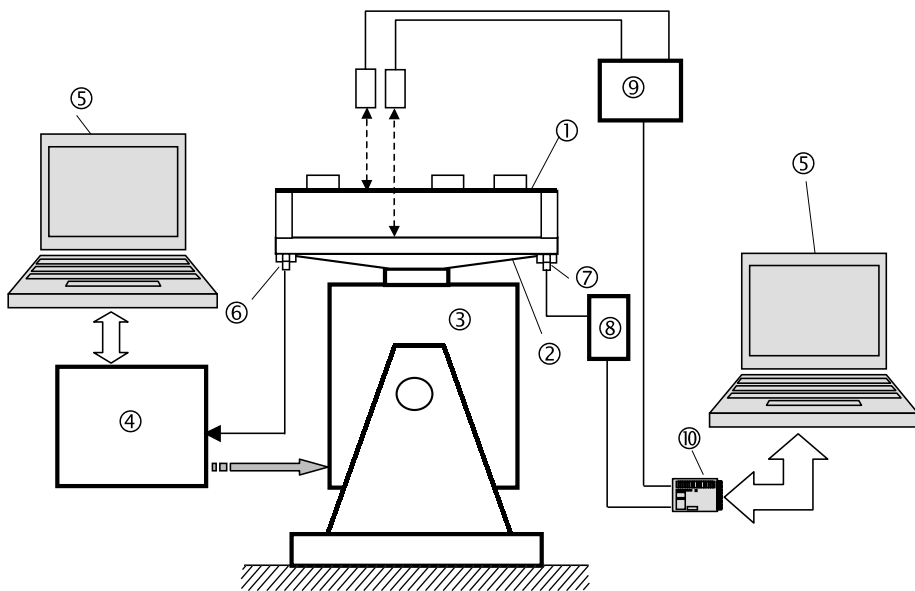


Figure 1. Schematics of the experimental rig.



Figure 2. Layout of the experimental rig.

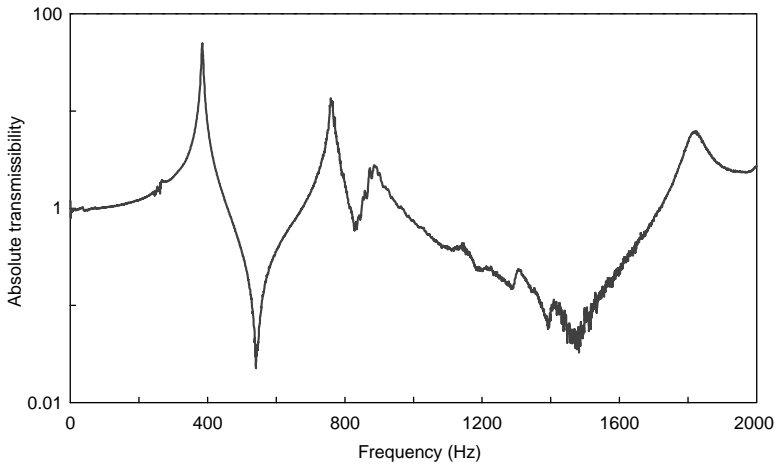


Figure 3. Experimentally measured universal absolute transmissibility of the PCB.

### 3. MODEL OF VIBRATION ISOLATED ELECTRONIC EQUIPMENT

Figure 5 shows the model of vibration isolated electronic enclosure (primary sub-system) containing the internally mounted PCB (secondary sub-system). The absolute deflections of the base, primary and secondary sub-system are  $y(t)$ ,  $x_p(t)$  and  $x_c(t)$ , respectively. The deflection of the primary sub-system relative to the base is  $z_p(t) = x_p(t) - y(t)$  and the deflection of the secondary sub-system relative to the primary sub-system is  $z_c(t) = x_c(t) - x_p(t)$ .

Typically, the mass of the secondary sub-system is negligibly small as compared with that of the primary one. Therefore, for simplicity, one now neglects the influence of the

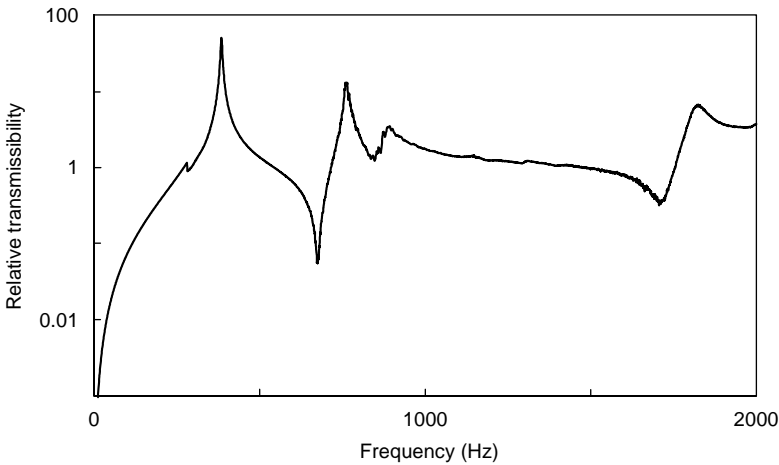


Figure 4. Experimentally measured universal relative transmissibility of the PCB.

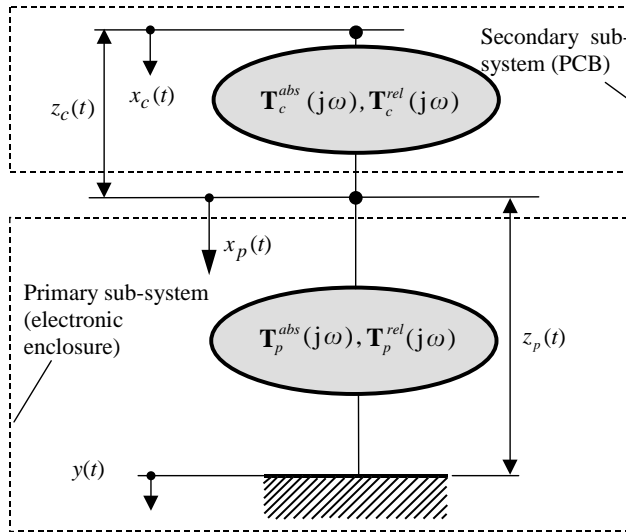


Figure 5. Simplified model of vibration isolated electronic enclosure containing the internally mounted PCB.

secondary sub-system on the dynamic response of the primary sub-system. In this approach, the vibration of the primary sub-system may be thought of as the vibrational input for the secondary sub-system. Hence, the dynamics of such a compound system may be analysed separately using individual complex transmissibilities of the primary and the secondary sub-systems.

In Figure 5, the complex universal absolute and relative transmissibilities,  $\mathbf{T}_c^{abs}(j\omega)$  and  $\mathbf{T}_c^{rel}(j\omega)$ , define the dynamic properties of the separated internal component. These functions were estimated experimentally in section 3. The universal absolute complex transmissibilities,  $\mathbf{T}_p^{abs}(j\omega)$  and  $\mathbf{T}_p^{rel}(j\omega)$ , define the dynamic properties of the vibration isolated electronic enclosure.

Let the normally distributed wideband random base acceleration be given by the power spectral density (PSD),  $S_{\ddot{y}}(\omega)$ . Using the universal absolute and relative complex transmissibilities of the primary sub-system,  $\mathbf{T}_p^{abs}(j\omega)$  and  $\mathbf{T}_p^{rel}(j\omega)$ , we find for the PSD of absolute acceleration and relative deflection of the primary sub-system [23]

$$S_{\ddot{x}_p}(\omega) = \left| \mathbf{T}_p^{abs}(j\omega) \right|^2 S_{\ddot{y}}(\omega), \quad S_{z_p}(\omega) = 1/\omega^4 \left| \mathbf{T}_p^{rel}(j\omega) \right|^2 S_{\ddot{y}}(\omega) \quad (1, 2)$$

Considering the vibration of the primary sub-system as the vibration input to the secondary sub-system and using universal absolute and relative complex transmissibilities of the secondary sub-system,  $\mathbf{T}_c^{abs}(j\omega)$  and  $\mathbf{T}_c^{rel}(j\omega)$  (as experimentally obtained in section 3), one finds for the PSD of absolute acceleration and relative deflection of the secondary sub-system

$$S_{\ddot{x}_c}(\omega) = \left| \mathbf{T}_c^{abs}(j\omega) \right|^2 S_{\ddot{x}_p}(\omega), \quad S_{z_c}(\omega) = 1/\omega^4 \left| \mathbf{T}_c^{rel}(j\omega) \right|^2 S_{\ddot{x}_p}(\omega). \quad (3, 4)$$

For the primary sub-system the root mean square (r.m.s.) value of absolute acceleration and relative deflection may be calculated by the integration [23]

$$\sigma_{\ddot{x}_p} = \sqrt{\frac{1}{2\pi} \int_{-\infty}^{\infty} S_{\ddot{x}_p}(\omega) d\omega}, \quad \sigma_{z_p} = \sqrt{\frac{1}{2\pi} \int_{-\infty}^{\infty} S_{z_p}(\omega) d\omega}. \quad (5, 6)$$

Similarly, for the secondary sub-system,

$$\sigma_{\ddot{x}_c} = \sqrt{\frac{1}{2\pi} \int_{-\infty}^{\infty} S_{\ddot{x}_c}(\omega) d\omega}, \quad \sigma_{z_c} = \sqrt{\frac{1}{2\pi} \int_{-\infty}^{\infty} S_{z_c}(\omega) d\omega}. \quad (7, 8)$$

In the first approximation, one considers that the fatigue accumulated by the sensitive internal PCB is proportional to the r.m.s. value of the relative deflection or absolute acceleration. By accounting for these dynamic responses of the internally mounted PCB as quantities to be minimized, the optimal problem may be stated

$$\sigma_{\ddot{x}_c} \rightarrow \min, \quad z_p^{peak} \leq \Delta; \quad \text{or} \quad \sigma_{z_c} \rightarrow \min, \quad z_p^{peak} \leq \Delta,$$

where  $\Delta$  is the allowed peak deflection (rattlespace) of the electronic box relative to the base. This value is defined primarily by the mechanical properties of the electrical harnesses and thermal interface and also by the properties of vibration isolators used.

For the normally distributed processes the peak deflection with the probability of 99.7% may be estimated using the  $3\sigma$  rule [1] as

$$z_p^{peak} = 3\sigma_{z_p}. \quad (9)$$

The optimization procedure is based on equations (2), (3), (4), (7) and (8) and the experimentally obtained dynamic properties of the PCB (universal absolute and relative transmissibilities, as described above). As a matter of fact, this approach yields the vibration isolator, which is optimally suited for the particular PCB.

#### 4. VIBRATION ISOLATION OF ELECTRONIC PACKAGE IN ZERO-G ENVIRONMENT

Given are the uniform PSD of the base acceleration  $S_{\ddot{y}}(\omega) = S_0 = 0.1g^2/\text{Hz}$  in the frequency range from 0 to 2000 Hz (overall level  $14g$  r.m.s.) and the allowable peak deflection of the electronic package relative to the base  $\Delta = 0.5$  mm.

**Problem.** Estimate the optimal properties of the isolator to minimize the r.m.s. level of absolute acceleration,  $\sigma_{\ddot{x}_c}$ , and relative deflection,  $\sigma_{z_c}$ , of the PCB, subject to restraint

imposed on peak relative deflection of the entire electronic package  $z_p^{peak}$  expressed as

$$\sigma_{\ddot{x}_c}, \sigma_{z_c} \rightarrow \min, z_p^{peak} \leq \Delta. \quad (10)$$

In the first approximation, the universal absolute complex transmissibility of the linearized single-degree-of-freedom (s.d.o.f.) isolator might be taken to be in the form

$$\mathbf{T}_p^{abs}(j\omega) = (\Omega_p^2 + 2j\omega\Omega_p\zeta_p)/(\Omega_p^2 - \omega^2 + 2j\omega\Omega_p\zeta_p), \quad (11)$$

where  $\Omega_p$  and  $\zeta_p$  are the linearized natural undamped frequency and loss factor of the isolator,  $\omega$  is the angular frequency and  $j = \sqrt{-1}$ .

Hence,

$$\mathbf{T}_p^{rel}(j\omega) = \mathbf{T}_p^{abs}(j\omega) - 1 = \omega^2/(\Omega_p^2 - \omega^2 + 2j\omega\Omega_p\zeta_p). \quad (12)$$

Since it is assumed that a light internal critical component does not affect the dynamic response of the relatively heavy electronic enclosure, the PSD of the absolute acceleration and this of the relative deflection of the isolator are per (3) and (4), where the appropriate universal transmissibilities are per (11) and (12).

By considering equations (11), (12) and the tables in reference [22] one find for the variances

$$\sigma_{\ddot{x}_p}^2 = \frac{S_0}{2\pi} \int_0^\infty |\mathbf{T}_p^{abs}(j\omega)|^2 d\omega = \frac{S_0}{2\pi} \int_0^\infty \left| \frac{\Omega_p^2 + 2j\omega\Omega_p\zeta_p}{\Omega_p^2 - \omega^2 + 2j\omega\Omega_p\zeta_p} \right|^2 d\omega = \frac{S_0\Omega_p}{4} \left( \frac{1}{2\zeta_p} + 2\zeta_p \right). \quad (13)$$

$$\sigma_{z_p}^2 = \frac{S_0}{2\pi} \int_0^\infty \frac{1}{\omega^4} |\mathbf{T}_p^{rel}(j\omega)|^2 d\omega = \frac{S_0}{2\pi} \int_0^\infty \frac{d\omega}{|\Omega_p^2 - \omega^2 + 2j\omega\Omega_p\zeta_p|^2} = \frac{S_0}{8\Omega_p^3\zeta_p}. \quad (14)$$

From equations (10) and (14), using the  $3\sigma$  rule, one finds

$$z_p^{peak} = 3\sigma_{z_p} = \sqrt{9S_0/8\Omega_p^3\zeta_p} = \Delta. \quad (15)$$

From equation (15), one expresses the required value of the natural frequency of the vibration isolator as a function of the loss factor at given intensity of the excitation,  $S_0$ , and allowable rattle space,  $\Delta$ , in the form

$$\Omega_p = 3\sqrt{9S_0/8\zeta_p\Delta^2}. \quad (16)$$

The numerical procedure, which is based on equations (1–8) and (16), is than applied. Figure 6 shows the superimposed dependencies of the r.m.s. values of relative deflection and absolute acceleration of the PCB on the value of loss factor of the vibration isolator. It is seen that these r.m.s. values reach simultaneously the minimum at almost the same value of the loss factor, namely,  $\zeta_p = 0.27$ . From equation (16), the optimal value for the natural frequency of the primary isolator is 87 Hz.

With such a vibration isolator, for the primary sub-system one finds

$$\sigma_{\ddot{x}_p} = 5.7g \text{ r.m.s.} \quad \text{and} \quad \sigma_{z_p} = 0.17 \text{ mm r.m.s.} \quad (17)$$

From equation (17), using the  $3\sigma$  rule, one finds that  $z_p^{peak} = 3\sigma_{z_p} \approx 0.5 \text{ mm}$ .

For the secondary sub-system (PCB), one finds

$$\sigma_{\ddot{x}_c} = 8.3g \text{ r.m.s.} \quad \text{and} \quad \sigma_{z_c} = 0.104 \text{ mm r.m.s.} \quad (18)$$

It is important to note, that in the case of the rigid mounting of the electronic box, for the dynamic responses of PCB one obtains

$$\sigma_{\ddot{x}_c} = 5.1g \text{ r.m.s.} \quad \text{and} \quad \sigma_{z_c} = 0.74 \text{ mm r.m.s.} \quad (19)$$

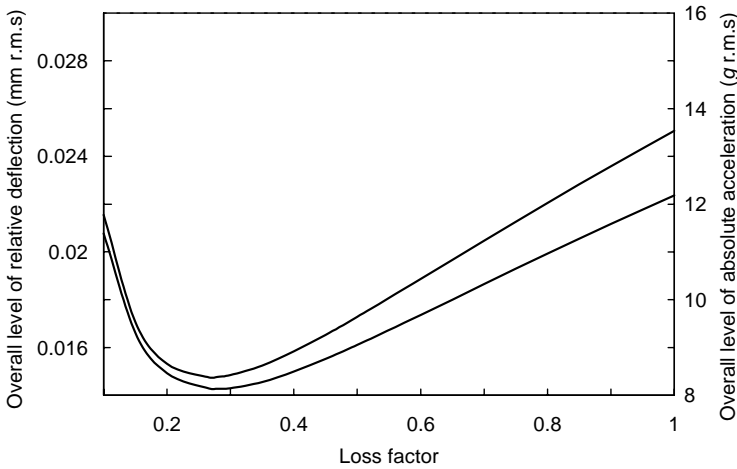


Figure 6. Dependencies of overall r.m.s. of relative deflection (lower curve) and absolute acceleration (upper curve) on the value of the loss factor of the primary vibration isolator.

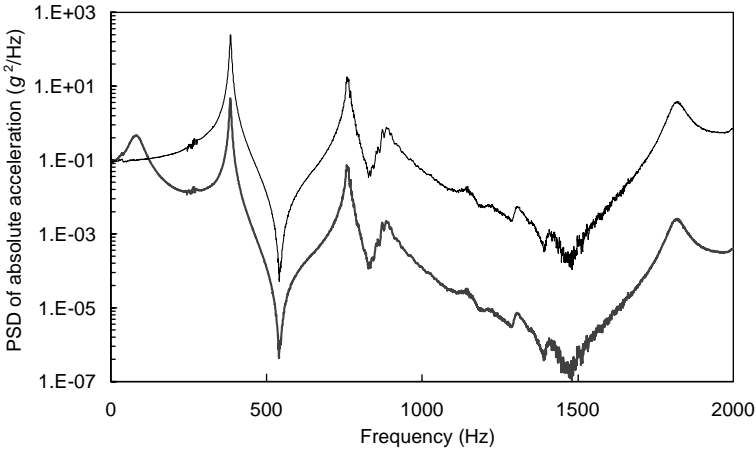


Figure 7. Comparison of PSD of absolute acceleration of the PCB in the cases of the rigidly mounted (upper curve) and vibration isolated (lower curve) electronic box.

From equations (18) and (19), the overall r.m.s. levels of dynamic responses of the PCB are reduced by a factor of 6.1 for absolute acceleration and 5.3 for relative deflections, when compared with the case of the rigid mounting of electronic box.

Figures 7 and 8 compare the PSD of absolute acceleration and relative deflection of the PCB in the cases of rigidly mounted and optimally isolated electronic box.

From Figures 7 and 8, the vibration isolated system shows essential vibration suppression in the entire frequency range with the exception of the narrow band 0–120 Hz, where insignificant amplification is due to the vibration isolator. However, this amplification is small since the vibration isolator is sufficiently damped. On the other hand, starting from the frequency of approximately 300 Hz, the vibration isolator provides for the dynamic response of PCB to be essentially reduced. Since the objective of the vibration isolator is to minimize the overall r.m.s. response of PCB in terms of absolute



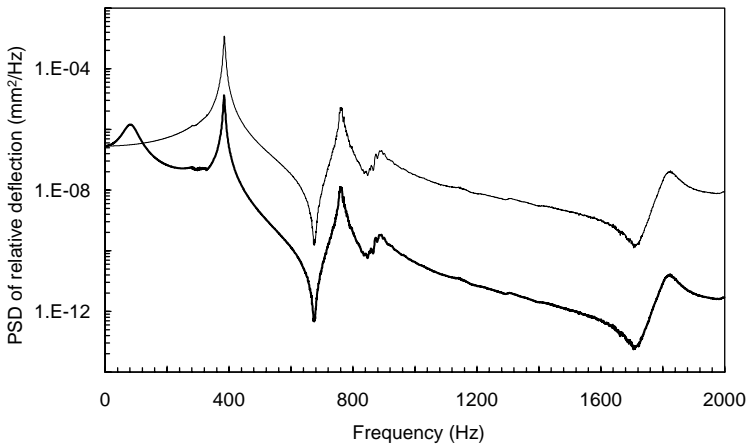


Figure 8. Comparison of PSD of relative deflection of the PCB in the cases of the rigidly mounted (upper curve) and vibration isolated (lower curve) electronic box.

acceleration and relative deflection, the local amplification at low frequencies is not critical.

## 5. VIBRATION ISOLATION OF ELECTRONIC PACKAGE IN HIGH-G ENVIRONMENT

The statement of the optimal problems for high-G airborne and space-borne environment is quite similar to that in zero-G environments, as considered above. The only difference is that the static deflection,  $\sigma$ , which arises due to the  $g$ -loading must be added on the top of the peak value of relative deflection obtained (see section 4):

$$z_p^{peak} = 3\sigma_{z_p} + \delta, \quad (20)$$

where  $\delta = G/\Omega_p^2$  is the static deflection due to the constant acceleration  $G$ .

Hence, instead of equation (15) we obtain

$$z_p^{peak} = 3\sigma_{z_p} + \delta = \sqrt{9S_0/8\Omega_p^3\zeta_p} + G/\Omega_p^2 = \Delta. \quad (21)$$

From equation (21), one obtains the relationship between the natural frequency and loss factor of vibration isolator at given intensity of excitation  $S_0$  and allowable rattle space  $\Delta$

$$\zeta_p = (9S_0/8)\Omega_p / (\Delta\Omega_p^2 - G)^2. \quad (22)$$

## 6. SENSITIVITY

The preceding analysis shows that the performance of the vibration isolator system depends strongly on the correct choice of its properties. However, from Figure 6, a reasonably small variation in the properties of the isolator about its optimal values does not lead to the drastic degradation in the overall performance.

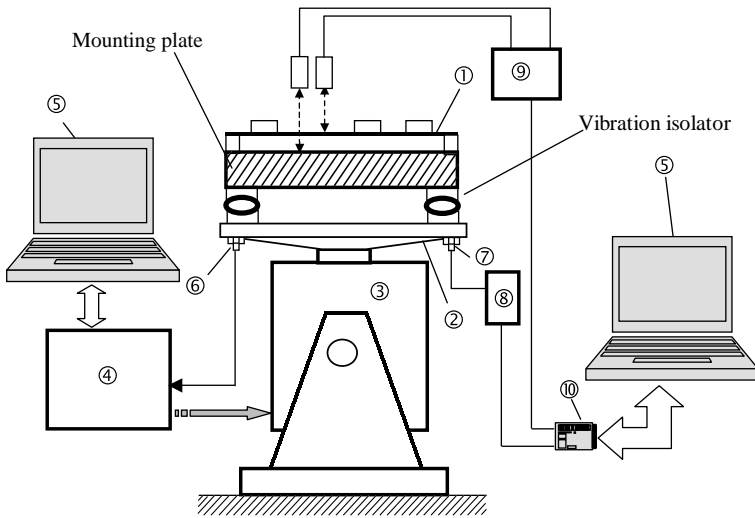


Figure 9. Schematics of experimental rig.

## 7. CHOICE OF VIBRATION ISOLATOR

Since the performance of the vibration protection system varies with the properties of the primary isolator, the designer must pay careful attention to the persistence of the above properties in the given temperature range and over the service life.

It is known that the widely used soft elastomeric mounts tend to stiffen and gain damping at low temperatures and to soften and lose damping at elevated temperatures. These variations may alter the vibration amplification near resonance and the “rattle room” along with the behaviour of the mounts near the end of their travel where highly non-linear stops can generate high-frequency vibrations which might be capable of exciting excessively the resonant modes of the internal sensitive components. That makes it practically impossible to keep optimized configuration in actual airborne applications.

Most probably, the all-metal isolators, such as military approved Shock Tech Cable or Wire Mesh Mounts<sup>¶</sup> or Metal & Mesh Mounts<sup>||</sup> (MET-L-FLEX Bushings), are the only feasible solutions. These are especially designed to withstand the severe environmental conditions while showing the persistence of parameters in a wide temperature range ( $-400^{\circ}\text{F}$  to  $+700^{\circ}\text{F}$ , typically), as compared with polymer isolators [12, 13, 24]. They provide consistent performance over temperature and time and offer suitable damping.

## 8. EXPERIMENTAL VALIDATION

Figure 9 shows the schematics of the experimental rig and instrumentation which is similar to that in Figure 1. As distinct from Figure 1, in this case the PCB is mounted upon the massive mounting plate (5 kg, approximately), which simulates the mass of the electronic package. This plate is supported from the shaker fixture by the two similar

<sup>¶</sup> <http://www.shocktech.com/isolatormounts.htm#Anchor-wiremesh>

<sup>||</sup> <http://www.barrymounts.com>

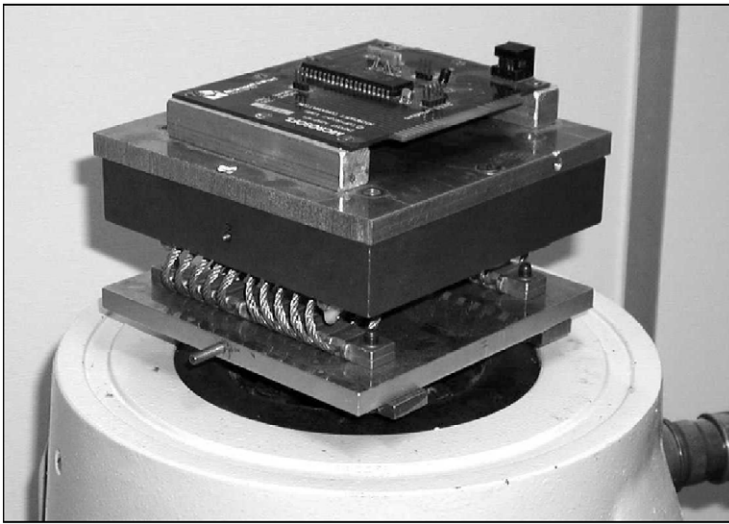


Figure 10. Experimental rig.

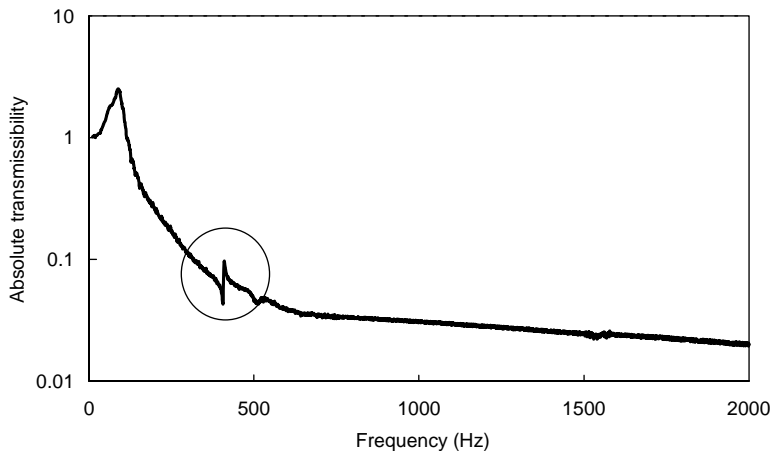


Figure 11. Absolute transmissibility of the primary isolator.

Shock-Tech cable-mounts with properties to obtain the natural frequency and loss factor in accordance with the optimal design of section 4. Figure 10 shows the detailed layout of the experimental rig.

From the optimal design, the primary vibration isolator has to provide for the modal parameters follow

$$\zeta_p^{opt} = 0.27 \quad \text{and} \quad \Omega_p^{opt}/2\pi = 87 \text{ Hz.}$$

Since wire-rope vibration isolators show well-pronounced non-linear properties, the experimentation was carried out at the full level of excitation 14 *g*.r.m.s. The inertial properties of the mounting plate and visco-elastic properties of vibration isolators were matched to obtain the required loss factor and natural frequency.

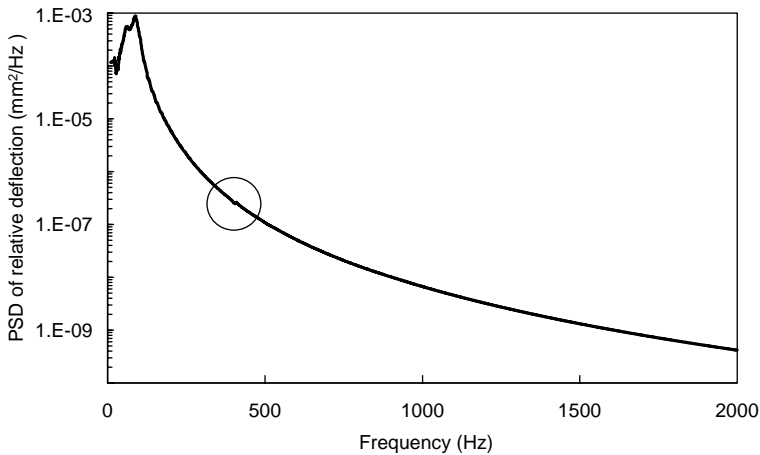


Figure 12. Experimentally measured PSD of the relative deflection of the vibration isolator.

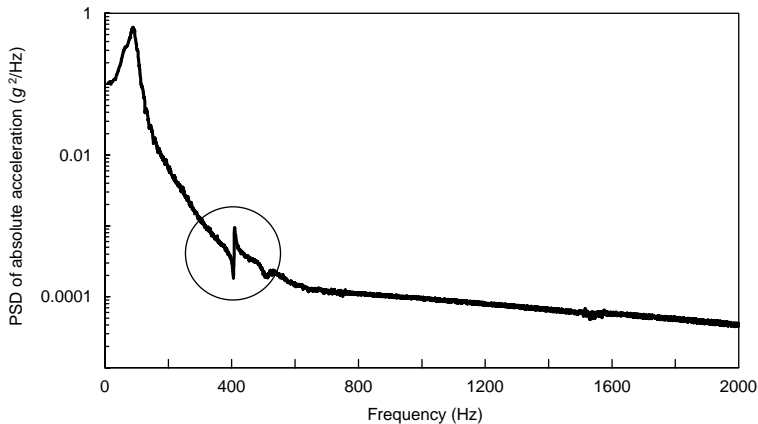


Figure 13. Experimentally measured PSD of the absolute acceleration of the vibration isolator.

Figure 11 shows the absolute transmissibility of the primary system. The s.d.o.f. curve-fitting procedure as applied to the above transmissibility yields the modal parameters  $\zeta_p = 0.23$  and  $\Omega_p/2\pi = 85.8$  Hz which are fairly close to the desired values. The encircled portion of the frequency response function (see also Figures 12 and 13) shows the characteristic anti-resonance/resonance sequence indicating the influence of the PCB upon the dynamic response of the primary vibration isolator. However, since the mass ratio is small, this influence is negligible, as it was assumed above.

Figure 12 shows the experimentally measured vibration response of the primary isolator in terms of PSD of relative deflection, indicating the overall level to be 0.2 mm r.m.s. (compare with 0.17 mm r.m.s. in analytical prediction).

Figure 13 shows the experimentally measured vibration response of the primary isolator in terms of PSD of absolute acceleration, indicating the overall level to be 5.6 g r.m.s. (compare with 5.7 g r.m.s. in analytical prediction).

Figure 14 shows the experimentally measured vibration response of the PCB in terms of PSD of relative deflection, indicating the overall level to be 0.012 mm r.m.s. (compare with

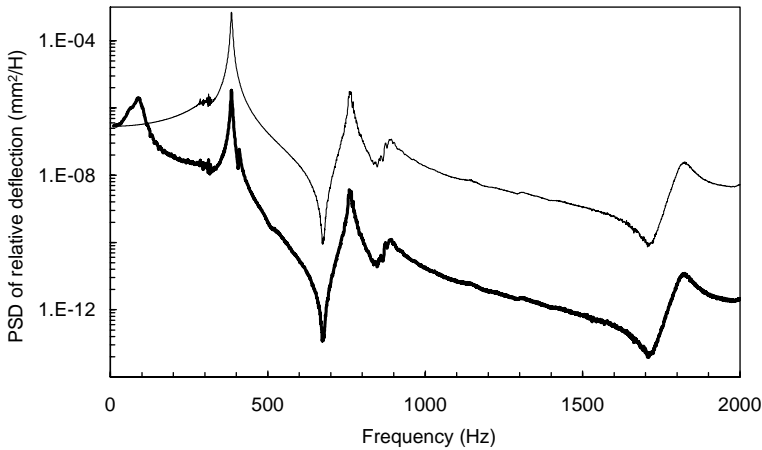


Figure 14. Experimentally measured PSD of the relative deflection of the PCB, upper curve for the rigidly mounted case and the lower curve for the isolated case.

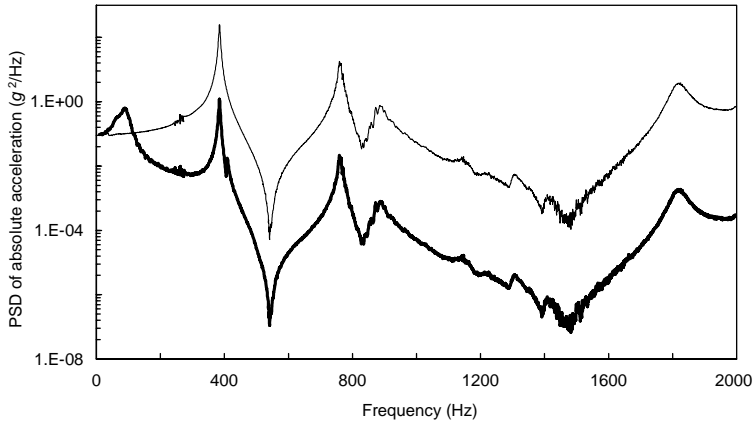


Figure 15. Experimentally measured PSD of the absolute acceleration of the PCB, the upper curve showing the rigidly mounted case and the lower curve is isolated results.

0.14 mm r.m.s. in analytical prediction). For comparison, the superimposed dynamic response of the rigidly mounted PCB shows overall level of relative deflection  $\sigma_{z_c} = 0.074$  mm. r.m.s.

Figure 15 shows the experimentally measured vibration response of the PCB system in terms of the PSD of absolute acceleration, indicating the overall level to be  $\sigma_{\ddot{x}_c} = 6.4$  g r.m.s. (compare with  $\sigma_{\ddot{x}_c} = 8.3$  g r.m.s. in analytical prediction). For comparison, the superimposed dynamic response of the rigidly mounted PCB shows overall level of relative deflection  $\sigma_{z_c} = 51$  g r.m.s..

The better performance of the vibration isolator (as compared with the analytical prediction) is obtained, however, because of the slightly increased rattle-space.

Figures 16 and 17 show superimposed experimental and analytically predicted dynamic responses of the vibration isolated PCB, which are in fair agreement.

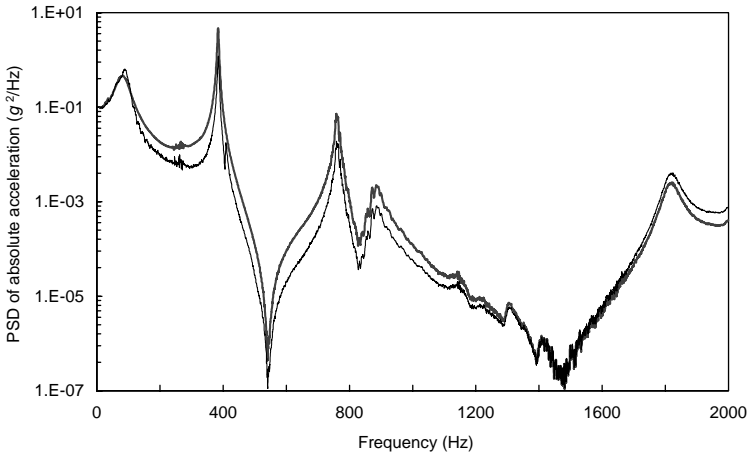


Figure 16. Comparison of the experimentally measured and analytically predicted PSD of the absolute acceleration of the PCB.

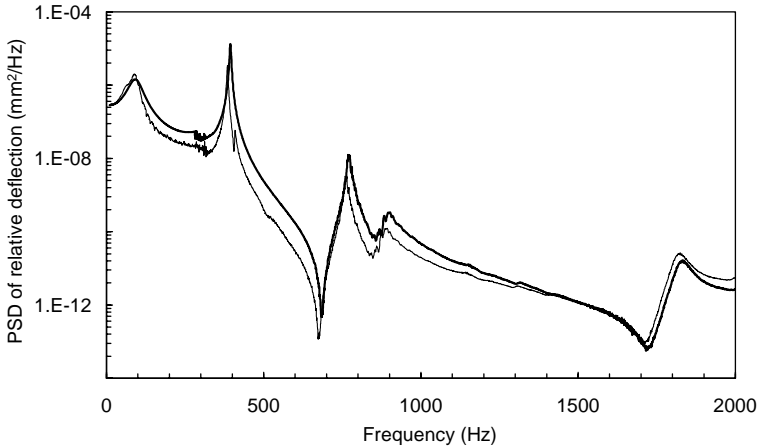


Figure 17. Comparison of the experimentally measured and analytically predicted PSD of the relative deflection of the PCB.

## 9. CONCLUSIONS

The article proposes a novel design approach to a vibration isolation of electronic equipment operating in harsh environmental conditions. By considering the dynamic properties and responses of the critical internal components, the model of the object of vibration protection is enhanced. The optimally chosen elastic and damping properties of the vibration isolators allow vibration experienced by these above internal components to be minimized, subject to restraints imposed on the peak deflections of the electronic box. The effectiveness of this approach is demonstrated analytically and experimentally.

The proposed approach yields the vibration isolator, which is optimally suited for the particular sensitive component. Further efforts should be aimed at enhancing the model of the vibration isolated enclosure and development of the design approaches to optimal vibration isolation of electronic equipment comprising multiple sensitive components.

## REFERENCES

1. J. L. SLOAN, 1985 *Design and Packaging of Electronic Equipment*. New York: Van Nostrand Reinhold Company.
2. D. S. STEINBERG 1988 *Vibration Analysis for Electronic Equipment*. New York: John Wiley & Sons, Inc.
3. J. W. DALLY 1990 *Packaging of Electronic Systems (A mechanical Engineering Approach)*. New York: McGraw-Hill Publishing Company.
4. THALES COMPUTERS 1997 *The Ruggedizer White Paper*, [http://www.cetia.com/product/prod\\_rug.htm](http://www.cetia.com/product/prod_rug.htm).
5. DY4 Systems Inc. 2001 *Ruggedization Levels*, <http://www.dy4.com/dy4/experience/rugglevels.htm>,
6. W. ANDREWS 2000 *COTS Journal* January/February. Good grades for COTS initiative, editorial, <http://www.rtcgroup.com/cotsjournal/janfeb2000/>.
7. D. OSADCA 2001 *COTS Journal* May. Future of harsh environment and mission-critical COTS, <http://www.rtcgroup.com/cotsjournal/may2001/>.
8. B. KROEGER 1997 *Texas Instruments Future Direction [COTS]*, [http://www.ti.com/sc/docs/products/military/cots\\_pem/index.htm](http://www.ti.com/sc/docs/products/military/cots_pem/index.htm).
9. V. ROGOV 1998 *COTS Journal* September/October. Ruggedness and attenuation to operational environments ensures COTS systems usability, [http://www.zmicro.com/hot\\_news2.htm](http://www.zmicro.com/hot_news2.htm)
10. I. KOLLER 1999 *IDAN Shock Mount Isolation Vibration Study*, <http://www.rtdusa.com/shockmount.htm>
11. DIAMOND SYSTEMS CORPORATION *Can-Tainer<sup>TM</sup>, Rugged PCI104 Enclosure System*, <http://www.diamondsys.com/cantainer.htm>
12. J. V. DENTE, J. L. MCCUTCHEON and A. K. JAIN 1995 *ShockTech Reports*. Vibration qualification of commercial computers for use in military tactical environments, <http://www.shocktech.com/reports.html>.
13. S. S. SEGUIN and H. LEKUCH *Isolating COTS Equipment from Shock and Vibration*, <http://www.shocktech.com/shockVibCusAss.htm>.
14. D. V. BALANDIN, N. N. BOLOTNIK and W. D. PILKEY, 2000 *Applied Mechanics Review* **53**, 237–264. Optimal protection from impact and shock: theory and methods.
15. E. SEVIN and W. D. PILKEY 1971 *Optimum Shock and Vibration Isolation*. The Shock and Vibration Information Centre, US Department of Defence.
16. M. Z. KOLOVSKY 1999 *Nonlinear Dynamics of Active and Passive Systems of Vibration Protection*. Berlin: Springer-Verlag.
17. REFERENCE 1981 *Vibration in engineering*, K. V. FROLOV, editor, Vol. 6. Moscow: Mashinostroenie (in Russian).
18. E-A-R SPECIALTY COMPOSITES 1995 *Machine Design* September 60–61. Protecting Electronic Equipment from Shock and Vibration.
19. S. GRIFFIN, J. GUSSY, S. LANE, A. STEVEN, B. HENDERSON and D. SCIULLI 2002 *American Society of Mechanical Engineers Journal of Vibration and Acoustics* **124**, 63–67. Virtual Skyhook vibration isolation System.
20. A. M. VEPRIK and V. I. BABITSKY 1999 *Proceedings of the 6th International Congress on Sound and Vibration*, Technical University of Denmark, Lyngby. Optimal external mounting for vibration protection of lightweight internal components of electronic equipment.
21. A. M. VEPRIK, V. I. BABITSKY, N. PUNDAK and S. RIABZEV 2001 *Journal of Shock and Vibration* **8**, 55–69. Vibration protection of critical components of infrared equipment.
22. A. M. VEPRIK and V. I. BABITSKY 2000 *Journal of Sound and Vibration* **238**, 19–30. Vibration protection of sensitive electronic equipment from harsh harmonic vibration.
23. S. H. CRANDALL and W. D. MARK 1963 *Random Vibration in Mechanical Systems*. New York: Academic Press.
24. E. JASSON 1999 *COTS Journal* July–August Shock and vibration isolators for COTS Equipment, <http://www.rtcgroup.com/cotsjournal/cotsjulyaugustp27.html>.